Published in "Current Biology 18(9): 678-683 , 2008"
which should be cited to refer to this work.

Regulation of Monoamine Oxidase A by Circadian-Clock Components Implies Clock Influence on Mood

Gabriele Hampp,[1] Jürgen A. Ripperger,[1] Thijs Houben,[2] Isabelle Schmutz,[1] Christian Blex,[3] Stéphanie Perreau-Lenz,[4] Irene Brunk,[3] Rainer Spanagel,[4] Gudrun Ahnert-Hilger,[3] Johanna H. Meijer,[2] and Urs Albrecht[1,*]

[1]Department of Medicine
Division of Biochemistry
University of Fribourg
1700 Fribourg
Switzerland
[2]Department of Molecular Cell Biology
Laboratory of Neurophysiology
Leiden University Medical Center
2300 RC Leiden
The Netherlands
[3]AG Functional Cell Biology
Center for Anatomy
Charité-Universitätsmedizin Berlin
10115 Berlin
Germany
[4]Department of Psychopharmacology
Central Institute of Mental Health
68159 Mannheim
Germany

Summary

The circadian clock has been implicated in addiction and several forms of depression [1, 2], indicating interactions between the circadian and the reward systems in the brain [3–5]. Rewards such as food, sex, and drugs influence this system in part by modulating dopamine neurotransmission in the mesolimbic dopamine reward circuit, including the ventral tegmental area (VTA) and the ventral striatum (NAc). Hence, changes in dopamine levels in these brain areas are proposed to influence mood in humans and mice [6–10]. To establish a molecular link between the circadian-clock mechanism and dopamine metabolism, we analyzed the murine promoters of genes encoding key enzymes important in dopamine metabolism. We find that transcription of the monoamine oxidase A (*Maoa*) promoter is regulated by the clock components BMAL1, NPAS2, and PER2. A mutation in the clock gene *Per2* in mice leads to reduced expression and activity of MAOA in the mesolimbic dopaminergic system. Furthermore, we observe increased levels of dopamine and altered neuronal activity in the striatum, and these results probably lead to behavioral alterations observed in *Per2* mutant mice in despair-based tests. These findings suggest a role of circadian-clock components in dopamine metabolism highlighting a role of the clock in regulating mood-related behaviors.

Results and Discussion

The Murine *Maoa* Promoter Is Regulated by Clock Components In Vitro

We analyzed the promoter of *Maoa* for presence of E-box elements. These elements serve as potential binding sites for heterodimers of CLOCK/BMAL1 or NPAS2/BMAL1, key components of the circadian-clock mechanism [11]. In the promoter of *Maoa*, we found E-box elements, which are conserved among mouse, rat, and human, suggesting comparable regulation of this gene in these species (Figure 1A). To determine whether the *Maoa* promoter is regulated by clock components, we cloned a 1.1 kb promoter fragment of the murine *Maoa* (*mMaoa*) gene containing one canonical and two noncanonical E-boxes into a luciferase reporter vector. Cotransfection with clock components of this reporter construct into the neuroblastoma cell line NG108-15 revealed regulatory effects of clock proteins on the *mMaoa* promoter (Figure 1B) in a concentration-dependent manner (Figure S1A available online). Surprisingly, CLOCK/BMAL1 does not activate the *mMaoa* promoter in the neuroblastoma cell line (Figure 1B) but in COS-7 monkey kidney cells (Table S1), suggesting a possible involvement of cell-type-specific cofactors in this process. Cotransfection of *Cry1*, a clock component of the negative limb of the clock regulatory mechanism [12], dampened the activation by NPAS2/BMAL1 in neuroblastoma cells. Cotransfection of *Per2* resulted in increased activation (Figure 1B) as observed previously for the activation of the *aminolevulinate synthase 1* promoter [13]. To test whether the conserved classical E-box is of importance in the *mMaoa* promoter, we deleted it. This resulted in a shortened 0.7 kb promoter that was still activated by NPAS2/BMAL1, however in a strongly reduced manner, indicating functional importance of the most 5′ E-box in the 1.1 kb construct (Figures 1A and 1B). In contrast to *mMaoa*, neither a 1.2 kb fragment of the murine *monoamine oxidase B* (*mMaob*) promoter (Figure S1B) nor a 3.3 kb promoter fragment of the tyrosine hydroxylase, the rate-limiting enzyme in dopamine synthesis (data not shown), displayed comparable effects in our assays. Taken together, our experiments indicate that the *mMaoa* promoter is prone to specific regulation by clock components in vitro.

The *MaoA* Gene Is Hardwired Directly to the Circadian Oscillator

In order to test circadian functionality of the *mMaoa* promoter, we transfected the *mMaoa*-luciferase reporter construct into NG108-15 neuroblastoma cells and followed its expression by using real-time bioluminescence monitoring. After synchronization with dexamethasone [14], we monitored luciferase activity in the cell population over 4 days (Figure 1C and Figure S1C). We observed an ~24 hr oscillation of luciferase activity with the same phase as a control reporter construct containing four E-box elements derived from the clock-controlled *Dbp* gene [15]. Similar results were also obtained upon transfection of the construct into NIH 3T3 fibroblasts cells (Figure S1C). This indicates that the *mMaoa* promoter is capable of oscillating in a circadian fashion.

In a next step, we investigated the regulation of the *mMaoa* promoter in vivo. We wanted to know whether BMAL1 directly interacts with the *mMaoa* promoter in brain regions that express this gene. Chromatin immunoprecipitation with antibodies against BMAL1 revealed binding of this protein to the promoter of *mMaoa* in brain tissue containing the VTA (Figure 1D). This binding was also time dependent with

*Correspondence: urs.albrecht@unifr.ch

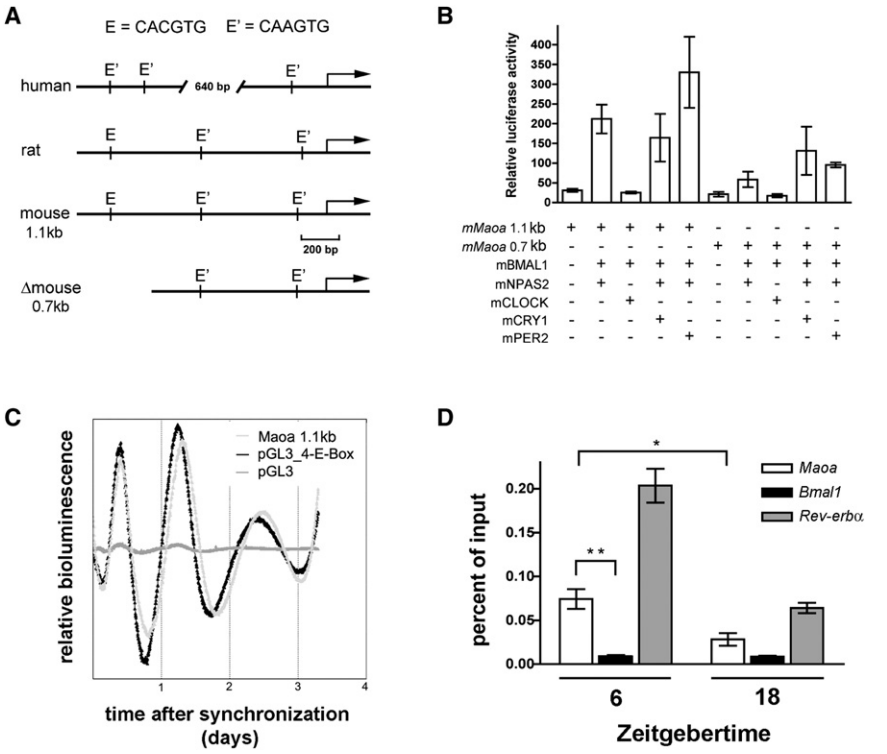

Figure 1. Regulation of the *mMaoa* Promoter by Clock Components

(A) Schematic representation of E-boxes conserved in human, rat, and mouse *Maoa* genes. Letters E and E' refer to sites of canonical and noncanonical E-box elements, respectively, serving as potential binding sites for the BMAL1-NPAS2 heterodimer. Arrows indicate the transcription start site.

(B) Transcriptional regulation of the *mMaoa* gene by clock components in NG108-15 cells. Luciferase reporter plasmids containing either a 1.1 kb *mMaoa* 5′ upstream region, including the three E-boxes (*Maoa* 1.1 kb) or a deletion of the canonical E-box (*Maoa* 0.7 kb) was used for the transcriptional assays. Presence (+) or absence (−) of the reporter and expression plasmids is shown. Each value represents the mean ± SD of three independent experiments with three replicates for each experiment.

(C) Circadian oscillations of luciferase reporter activity in dexamethasone synchronized NG108-15 cells. Detrended, normalized time series, each derived by averaging the bioluminescence profiles of two independent cultures (representative experiment out of three independent experiments), are shown. "pGL3" refers to a luciferase reporter (gray, negative control), "pGL3_4-E-box" refers to a pGL3 reporter containing four E-boxes of the *Dbp* promoter (black, positive control), "Maoa 1.1kb" refers to a pGL3 reporter containing a 1.1 kb promoter fragment of the mouse *Maoa* promoter (light-gray line).

(D) Binding of BMAL1 to the *mMaoa* promoter in mouse brain tissue collected at ZT 6 and ZT 18 as revealed by chromatin immunoprecipitation (ChIP). BMAL1 does not bind to its own promoter (black bars, negative control, $p > 0.05$, ZT 6 versus ZT 18) but binds in a time-dependent fashion to the *mRevErbα* promoter (gray bars, positive control, $p < 0.05$, ZT 6 versus ZT 18) and to the *mMaoa* promoter (white bars, $^{*}p < 0.05$ and $^{**}p < 0.01$). Each value represents the mean ± SEM of three independent experiments with the p values determined by the Student's t test.

significantly more BMAL1 binding at Zeitgeber time (ZT) 6 compared to ZT 18 ($p < 0.05$, t test) comparable to the time-dependent binding of BMAL1 to the promoter of *Rev-erbα*, a circadian-clock component (Figure 1D). The lower signal of BMAL1 binding at the *mMaoa* promoter in vivo probably reflects the fact that fewer cells in the analyzed brain region express *mMaoa* in a circadian manner as compared to the *Rev-erbα* gene. Binding of BMAL1 is not observed in the promoter region of the *mBmal1* gene, a circadian gene that does not regulate itself. BMAL1 binding at the *mMaoa* promoter was also not observed in the cortex region or the liver of the same animals (data not shown). We conclude that the *mMaoa* promoter can be regulated by BMAL1 in a time-dependent fashion in brain tissue containing the VTA.

Expression of *Maoa* Is Reduced in *Per2* Mutant Mice

Per2^{Brdm1} mutant mice display altered responses to drugs of abuse [2, 16], implying abnormal signaling in the mesolimbic dopaminergic system of these animals. Therefore, we investigated region-specific and time-dependent expression of *mMaoa* and *mMaob* in the mesolimbic system including the striatum and the VTA. We found cycling diurnal expression of *mMaoa* mRNA in the VTA of wild-type animals ($p < 0.01$, one-way ANOVA) with a maximum at ZT 6, whereas *mMaob* expression was not cycling diurnally (Figure 2A). No diurnal variation for both *mMaoa* and *mMaob* could be detected in *Per2*^{Brdm1} mutant mice having a defective circadian clock ($p > 0.05$, one-way ANOVA). Significantly lower mRNA levels of *Maoa* were observed in these animals at ZT 6 ($p < 0.05$, two-way ANOVA) (Figure 2A; for micrographs, see Figure S2). Diurnal expression for *mMaoa* was also observed in the ventral striatum (NAc) for both genotypes with reduced expression in *Per2*^{Brdm1} mutants at ZT 6 and ZT 12 ($p < 0.05$, two-way ANOVA), whereas *mMaob* expression was not diurnal (Figure 2B). However, *mMaob* expression was lower in *Per2*^{Brdm1} mutants at ZT 18 ($p < 0.01$, two-way ANOVA). These observations support our finding that the *mMaoa* promoter can be regulated by clock components and that PER2 probably plays a positive role in this mechanism by increasing the amplitude (Figures 1B, 2A, and 2B). The expression analyses presented above indicate that *mMaoa* mRNA is stronger expressed than *mMaob* in parts of the mesolimbic dopaminergic system, but we do not know whether this translates to the protein level.

MAOA Activity Is Reduced and Dopamine Levels Are Elevated in *Per2* Mutant Mice

Alterations in expression of *Maoa* mRNA in *Per2*^{Brdm1} mutant mice lead us to determine the total activity of MAO (MAOA and MAOB) in the VTA. We find that it follows the mRNA expression pattern of *mMaoa* with a maximum of MAO activity at ZT 6 and a significantly cycling diurnal variation in wild-type mice ($p < 0.05$, one-way ANOVA) but no variation ($p > 0.05$, one-way ANOVA) and reduced activity in *Per2*^{Brdm1} mutants ($p < 0.0001$, two-way ANOVA) (Figure 2C). In the striatum (composed of the caudate Putamen [CPu] and the NAc), to which the VTA projects, MAO activity was diurnal in wild-type mice ($p < 0.05$, one-way ANOVA). This activity was constant in *Per2*^{Brdm1} mutant animals ($p > 0.05$, one-way ANOVA). The maximum of activity was delayed to ZT 12 in wild-type animals (Figure 2D) compared to the maximal activity in the VTA (Figure 2C), and activity was significantly reduced at this

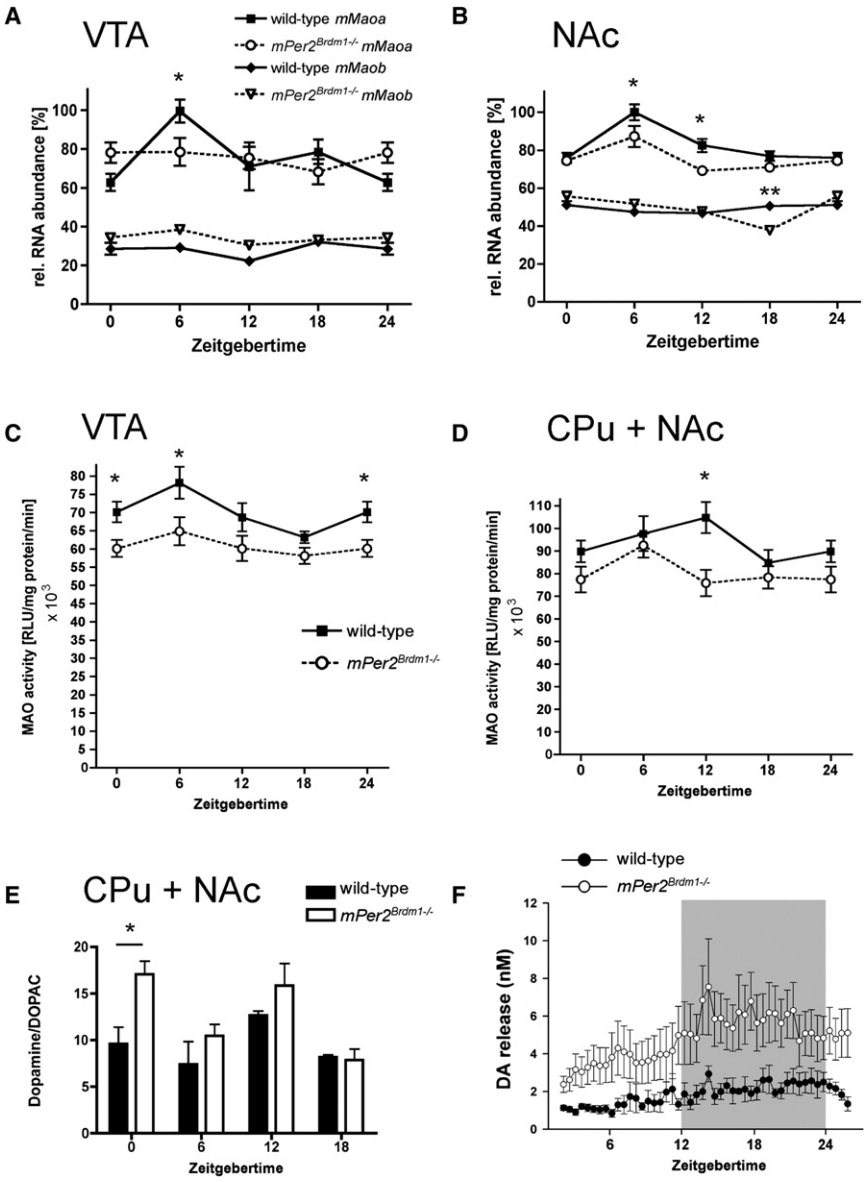

Figure 2. Expression of *mMaoa* and *mMaob*, MAO Activity, and Striatal Dopamine Levels in Wild-Type and *Per2*^{Brdm1} Mutant Mice

(A) mRNA expression of *mMaoa* (wild-type, black squares; *Per2*^{Brdm1} mutant, open circles) and *mMaob* (wild-type, black diamonds; *Per2*^{Brdm1} mutant, open triangles) in the VTA (n = 3 per genotype each). Two-way ANOVA with Bonferroni post test revealed for *mMaoa* a significant effect between the genotypes at ZT 6 (*p < 0.05) but no difference between genotypes for *mMaob* (p > 0.05). One-way ANOVA shows a significant variation of expression over time for *mMaoa* in wild-type mice (p < 0.01) and no variation in *Per2*^{Brdm1} animals (p > 0.05). No variation in time was observed in both genotypes for *mMaob* (p > 0.05). *mMaoa* was significantly more highly expressed than *mMaob* in both genotypes (p < 0.001).

(B) mRNA expression of *mMaoa* and *mMaob* in the ventral striatum (NAc) (n = 3 per genotype each). Two-way ANOVA with Bonferroni post test revealed for *mMaoa* a significant effect on genotype (p < 0.01) and time (p < 0.01) but no interaction between the two (p > 0.05). Significant differences between the genotypes at ZT 6 (*p < 0.05) and ZT 12 (*p < 0.05) were observed. For *mMaob*, a significant difference between genotypes was observed at ZT 18 (**p < 0.01). *mMaoa* was significantly more highly expressed than *mMaob* in both genotypes (p < 0.001).

(C) Enzymatic activity of MAO in the VTA (n = 3 per genotype). Two-way ANOVA revealed a significant effect on genotype (p < 0.0001) and time (p < 0.05) and no interaction between the two factors (p > 0.05). Bonferroni post test shows a significant difference between genotypes at ZT 6 (*p < 0.01) and ZT 0/24 (*p < 0.05). One-way ANOVA shows significant variation of enzyme activity over time in wild-type mice (p < 0.05) and no variation in *Per2*^{Brdm1} animals (p > 0.05).

(D) Enzymatic activity of MAO in the striatum (CPu + NAc) (n = 3 per genotype). Two-way ANOVA revealed a significant difference in genotype (p < 0.001) and time (p < 0.05) but no interaction between the two (p > 0.05). Bonferroni post test shows a significant difference between genotypes at ZT 12 (*p < 0.001). One-way ANOVA shows significant variation of enzyme activity over time in wild-type mice (p < 0.05) and no variation in *Per2*^{Brdm1} animals (p > 0.05).

(E) Dopamine/DOPAC ratio in the striatum (CPu + NAc). Two-way ANOVA revealed a significant difference in genotype (p < 0.05) and time (p < 0.01) but no interaction between the two (p > 0.05). Bonferroni post test shows a significant difference between genotypes at ZT 0/24 (*p < 0.05). Data for ZT 0 and ZT 24 are double plotted. Values represent the mean ± SEM.

(F) Extracellular levels of dopamine in the ventral striatum (NAc). *Per2*^{Brdm1} animals showed higher basal levels of dopamine release compared to wild-types (p < 0,05; two-way ANOVA for repeated-measures; genotype $F_{1, 9} = 5.4$). A diurnal rhythm was observed in *Per2*^{Brdm1} mice (p < 0.0001; one-way ANOVA; time $F_{47, 235} = 2.6$) as well as in wild-type littermates (p < 0.0001; one-way ANOVA; time $F_{47, 188} = 2.5$). Values represent the mean ± SEM (n = 5–6 per genotype).

time point in *Per2*^{Brdm1} mutant mice (Figure 2D) (p < 0.001, two-way ANOVA). The delay of maximal MAO activity in the striatum compared to maximal *mMaoa* mRNA expression in the ventral striatum (NAc) might be the result of MAO activity in the CPu contributing, besides the NAc, to the total activity in the striatum. However, it appears that the reduced expression levels of *mMaoa* in *Per2*^{Brdm1} mutants are reflected in the total MAO activity, indicating that in the mouse striatum, dopamine is metabolized predominantly by MAOA under basal conditions. This is consistent with previous findings in *Mao*-deficient mice [17, 18]. Taken together, our observations indicate that loss of functional PER2 lowers activity of MAO, which appears to be the result of reduced expression of *mMaoa*. Because dopamine is the most prominent neurotransmitter in the NAc of the striatum, we expected an increase in the dopamine to DOPAC ratio in this region of the brain. We found that this ratio was significantly elevated in the striatum (CPu and NAc) of *Per2*^{Brdm1} mutant mice (p < 0.05, two-way ANOVA) (Figure 2E). This is consistent with our finding that MAO activity is reduced. To investigate whether this increase can be observed extracellularly, we performed microdialysis in the ventral striatum (NAc). We find that under basal conditions, dopamine release is significantly increased in *Per2*^{Brdm1} mutant animals compared to wild-type littermates (p < 0.05; two-way ANOVA). Furthermore, we observed in both genotypes diurnal changes in the levels of this neurotransmitter;

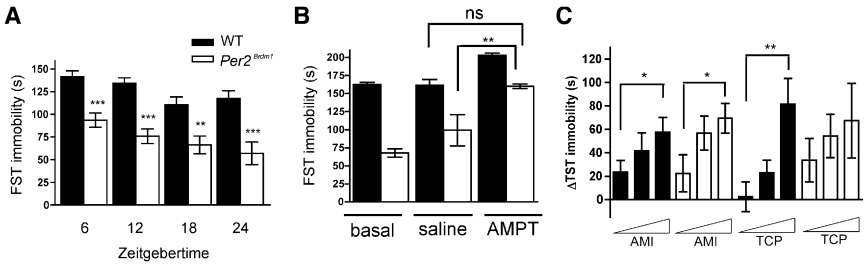

Figure 3. Depression-Resistant-like Phenotype in *Per2*^{Brdm1} Mutant Mice and Relation to MAO

(A) Comparison of immobility in the forced-swim test (FST) between wild-type (black bars) and *Per2*^{Brdm1} mutant mice (white bars) at different times (n = 6–14 per genotype). Two-way ANOVA shows a significant effect on genotype ($p < 0.0001$) but not on time ($p > 0.05$) and no interaction between these two factors ($p > 0.05$). One-way ANOVA with Bonferroni's multiple-comparison test reveals significant differences between the genotypes at all time points (**$p < 0.01$, ***$p < 0.001$).

(B) Rescue of the depression-resistant-like phenotype assessed by FST in *Per2*^{Brdm1} mutant mice by blocking tyrosine hydroxylase activity with alpha-methyl-p-tyrosine (AMPT) at ZT 6. A Student's t test reveals significant differences after AMPT treatment (200 mg/kg) in *Per2*^{Brdm1} mutant mice compared to basal levels and saline treatment (**$p < 0.01$, n = 9–12) but no significant difference (ns) to saline-treated wild-type animals.

(C) Decrease in immobility at ZT 6. Tail-suspension test (TST) performed 30 min after saline injection and the subsequent day 30 min after drug treatment with amitriptyline (AMI) and tranylcypromine (TCP). Concentrations used for AMI were 3, 6, and 9 mg/kg body weight and for TCP 6, 9, and 12 mg/kg body weight (n = 11–18). A Student's t test revealed significant differences between the lowest and the highest dose for the AMI treatment in both genotypes (*$p < 0.05$). For TCP treatment, only wild-type mice show a significant difference between the lowest and the highest dose (**$p < 0.01$). This is not the case for *Per2*^{Brdm1} mutant mice, indicating the higher sensitivity of these animals to TCP. Values represent the mean ± SEM.

these changes are in opposite phases as compared to MAO activity in the same brain region. We conclude that loss of functional PER2 is likely to lower MAOA activity in the striatum, contributing to increased dopamine levels in *Per2*^{Brdm1} mutant mice in this brain area. In contrast to *Maoa*-deficient mice that show aggressive behavior and elevated serotonin levels, we did not make these observations in *Per2*^{Brdm1} mutants (data not shown), probably because *Maoa* expression is not completely eliminated in our mutants. However, studies that associate human *MAOA* with alcoholism [19, 20] highlight a possible correlation between reduced expression of *mMaoa* in *Per2*^{Brdm1} mutants and increased ethanol intake in these animals [16].

Differences in Despair-Based Behavioral Tests between *Per2*^{Brdm1} Mutant and Wild-Type Mice

In humans, dopamine levels are related to mood [6]. Because *Per2*^{Brdm1} mutant mice display increased levels of this neurotransmitter in the striatum, we wanted to probe for behavioral alterations by applying despair-based behavioral tests believed to correlate with human mood disorders [21]. We examined wild-type and *Per2*^{Brdm1} mutant mice in the Porsolt forced-swim test (FST) and the tail-suspension test (TST). They measure the duration of immobility occurring after exposure of mice to an inescapable situation. However, they appear to be regulated by different sets of genes and hence may result in different outcomes [22]. These tests could be used because basal locomotor activity in the two genotypes is not different [2, 23]. The FST shows that *Per2*^{Brdm1} mutant mice display significantly less immobility compared to wild-type animals ($p < 0.0001$, two-way ANOVA, Figure 3A). This indicates an increase in neurotransmitter levels in *Per2*^{Brdm1} mutants. Because the response to cocaine [2] as well as expression and activity levels of *mMaoa* was highest at ZT 6 in the VTA, we performed all subsequent behavioral tests at ZT 6. To examine whether the lower immobility in *Per2*^{Brdm1} mutants is due to their elevated dopamine levels (Figure 2F), we aimed to diminish the amount of dopamine in these animals. We treated the mice with alpha-methyl-p-tyrosine (AMPT), a potent inhibitor of tyrosine-hydroxylase (TH), the rate-limiting enzyme of catecholamine synthesis, to reduce dopamine levels. We find that AMPT increased immobility in *Per2*^{Brdm1} mutants compared to saline-treated mutants ($p < 0.01$, t test), and immobility became comparable to saline-treated wild-type mice (nonsignificant difference [ns]; Figure 3B). We conclude that inhibition of TH leads to a behavioral rescue of *Per2*^{Brdm1} mutants in the FST (Figure 3B) indicating an involvement of dopamine (and/or other catecholamines) in this phenotype.

In TST, we find that immobility times are not different between the genotypes (Figure S3). Different outcomes in these despair-based behavioral tests for mice are not unusual [22]. However, because of the comparable behavioral baselines of the two genotypes, we could use the TST to titrate MAO activity with an inhibitor in the two genotypes. Because *Per2*^{Brdm1} mutants show less MAO activity (Figures 2C and 2D), we expected these animals to respond to lower doses of tranylcypromine (TCP), a MAO inhibitor. In comparison amitriptyline (AMI), a nonselective monoamine reuptake inhibitor mainly influencing serotonin and noradrenaline levels in the synaptic cleft should be effective at similar doses for both genotypes. We found these predictions to be met by intraperitoneal injections of AMI and TCP (Figure 3C). Both genotypes show a similar dose-dependent decrease in immobility for AMI, whereas *Per2*^{Brdm1} mutant mice are more sensitive to TCP. These experiments are in agreement with the observation that *mMaoa* expression and MAO activity is reduced in *Per2*^{Brdm1} mutants and therefore less inhibitor is necessary to abolish MAO function. Taken together, these findings indicate that *Per2*^{Brdm1} mutants react differently compared to wild-types in tests believed to correlate with human mood disorders.

Electrical Neuronal Activity Is Altered in *Per2* Mutant Mice in Response to MAO Inhibitors

To test how electrical activity is affected after treatment with AMI and TCP in wild-type and *Per2* mutant mice, we measured neuronal activity in the ventral striatum (NAc) in vivo. Multiunit activity recordings show that wild-type and *Per2*^{Brdm1} mutant animals react similarly to AMI (Figures 4A, 4B, and 4E). Interestingly, wild-type mice do not show altered activity traces after injection of 6 mg/kg TCP at ZT 6. In contrast, *Per2* mutant mice display a strong response visible in the change of the activity trace after TCP injection at ZT6 (Figures 4C and 4D). It appears that neuronal activity in *Per2* mutant mice is significantly affected compared to that in wild-type animals ($p < 0.05$, t test, Figure 4E). This result indicates that *Per2* mutants are more sensitive to TCP than wild-type mice. This might be the result of lower amounts of MAOA enzyme due to a reduced expression of the *mMaoa* gene (Figure 2). Hence,

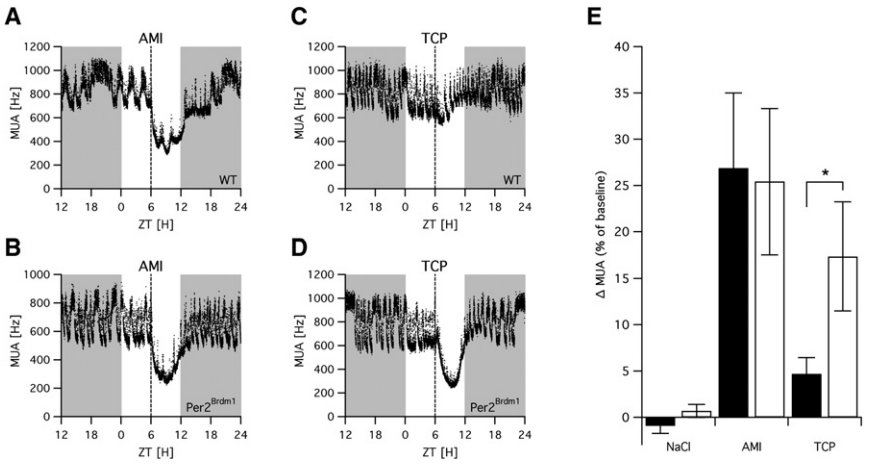

Figure 4. NAc Electrical Activity Responses to AMI and TCP Injections in Wild-Type and *Per2*^{Brdm1} Mutant Mice

(A–D) Raw data traces show the effect of AMI or TCP injection on multiple unit activity (MUA) in the NAc of wild-type (WT) and *Per2*^{Brdm1} mutant mice per 10 s. The gray background represents lights off, whereas the white background is lights on. Dotted lines indicate time of injection of 9 mg/kg body AMI or 6 mg/kg TCP. (A) shows the response to AMI in a WT animal. (B) shows the response to AMI in a *Per2*^{Brdm1} mutant mouse. (C) shows the response to TCP in a WT animal. (D) shows the response to TCP in a *Per2*^{Brdm1} mutant mouse.

(E) Comparison of the reduction of NAc firing rate in response to saline, AMI, and TCP injections between WT (black bars) and *Per2*^{Brdm1} mutant (white bars) mice (n = 8–11). TCP responses were significantly different between WT and *Per2*^{Brdm1} mutant mice (Student's t test, *p < 0.05). Values represent the mean ± SEM.

these mice are potentially useful to screen for drugs targeting MAOA to readjust intracerebral dopamine levels.

The behavioral and neuronal activity measurements for *Per2*^{Brdm1} mutant mice (Figures 3 and 4 and [2]) could also be explained by a change in the expression of the dopamine transporter (DAT) and changes in dopamine receptors (DR1 and DR2). This seems to be unlikely because expression of DAT is not significantly altered in *Per2*^{Brdm1} mutants (Figure S4). Furthermore, expression of the excitatory dopamine receptor DR1 is reduced, and expression of the inhibitory dopamine receptor DR2 is elevated (Figure S4). This indicates a compensatory response of the mutant organism to the elevated dopamine concentrations at the level of its receptors.

Conclusions

Taken together, our results indicate a direct influence of circadian-clock components on *mMaoa* expression and activity in the mesolimbic dopaminergic system. In particular, PER2 appears to act as a positive factor, and its absence leads to reduced *Maoa* expression and activity resulting in elevated dopamine levels in the ventral striatum (NAc). The behavioral alterations that are observed in *Per2* mutant mice with tests modeling human mood disorders are probably due to the elevated dopamine levels. This implies that alterations in the clock, as they occur in shift workers, pilots, and people suffering from jet-lag, may have profound consequences for brain function including mood regulation by the mesolimbic dopaminergic system.

Acknowledgments

We would like to thank Dr. S. McKnight and Dr. U. Schibler for reagents, Dr. John Reinhard, S. Baeriswyl-Aebischer, A. Hayoz, and G. Bulgarelli for technical assistance, and Dr. J.L. Dreyer, Dr. C. deVirgilio, and Dr. P. Lavenex for suggestions on the manuscript. This research was supported by the DFG SP383 (R.S.), the Velux Foundation (U.A.), the Swiss National Science Foundation (U.A.), and EUCLOCK (J.M. and U.A.).

References

1. Baird, T.J., and Gauvin, D. (2000). Characterization of cocaine self-administration and pharmacokinetics as a function of time of day in the rat. Pharmacol. Biochem. Behav. *65*, 289–299.
2. Abarca, C., Albrecht, U., and Spanagel, R. (2002). Cocaine sensitization and reward are under the influence of circadian genes and rhythm. Proc. Natl. Acad. Sci. USA *99*, 9026–9030.
3. Andretic, R., Chaney, S., and Hirsh, J. (1999). Requirement of circadian genes for cocaine sensitization in Drosophila. Science *285*, 1066–1068.
4. Yuferov, V., Kroslak, T., Laforge, K.S., Zhou, Y., Ho, A., and Kreek, M.J. (2003). Differential gene expression in the rat caudate putamen after "binge" cocaine administration: Advantage of triplicate microarray analysis. Synapse *48*, 157–169.
5. Sanchis-Segura, C., and Spanagel, R. (2006). Behavioural assessment of drug reinforcement and addictive features in rodents: An overview. Addict. Biol. *11*, 2–38.
6. Nestler, E.J., and Carlezon, W.A., Jr. (2006). The mesolimbic dopamine reward circuit in depression. Biol. Psychiatry *59*, 1151–1159.
7. Lüscher, C. (2007). Drugs of abuse. In Basic and Clinical Pharmacology, 10th Edition, B.G. Katzung, ed. (New York: McGraw Hill), pp. 511–525.
8. Andretic, R., and Hirsh, J. (2000). Circadian modulation of dopamine receptor responsiveness in Drosophila melanogaster. Proc. Natl. Acad. Sci. USA *97*, 1873–1878.
9. McClung, C.A., Sidiropoulou, K., Vitaterna, M., Takahashi, J.S., White, F.J., Cooper, D.C., and Nestler, E.J. (2005). Regulation of dopaminergic transmission and cocaine reward by the Clock gene. Proc. Natl. Acad. Sci. USA *102*, 9377–9381.
10. Roybal, K., Theobold, D., Graham, A., Dinieri, J.A., Russo, S.J., Krishnan, V., Chakravarty, S., Peevey, J., Oehrlein, N., Birnbaum, S., et al. (2007). Mania-like behavior induced by disruption of CLOCK. Proc. Natl. Acad. Sci. USA *104*, 6097–6098.
11. Liu, A.C., Lewis, W.G., and Kay, S.A. (2007). Mammalian circadian signaling networks and therapeutic targets. Nat. Chem. Biol. *3*, 630–639.
12. Wijnen, H., and Young, M.W. (2006). Interplay of circadian clocks and metabolic rhythms. Annu. Rev. Genet. *40*, 409–448.
13. Kaasik, K., and Lee, C.C. (2004). Reciprocal regulation of haem biosynthesis and the circadian clock in mammals. Nature *430*, 467–471.
14. Balsalobre, A., Brown, S.A., Marcacci, L., Tronche, F., Kellendonk, C., Reichardt, H.M., Schutz, G., and Schibler, U. (2000). Resetting of circadian time in peripheral tissues by glucocorticoid signaling. Science *289*, 2344–2347.
15. Ripperger, J.A., Shearman, L.P., Reppert, S.M., and Schibler, U. (2000). CLOCK, an essential pacemaker component, controls expression of the circadian transcription factor DBP. Genes Dev. *14*, 679–689.
16. Spanagel, R., Pendyala, G., Abarca, C., Zghoul, T., Sanchis-Segura, C., Magnone, M.C., Lascorz, J., Depner, M., Holzberg, D., Soyka, M., et al. (2005). The clock gene Per2 influences the glutamatergic system and modulates alcohol consumption. Nat. Med. *11*, 35–42.

17. Fornai, F., Chen, K., Giorgi, F.S., Gesi, M., Alessandri, M.G., and Shih, J.C. (1999). Striatal dopamine metabolism in monoamine oxidase B-deficient mice: A brain dialysis study. J. Neurochem. *73*, 2434–2440.
18. Cases, O., Seif, I., Grimsby, J., Gaspar, P., Chen, K., Pournin, S., Muller, U., Aguet, M., Babinet, C., Shih, J.C., et al. (1995). Aggressive behavior and altered amounts of brain serotonin and norepinephrine in mice lacking MAOA. Science *268*, 1763–1766.
19. Vanyukov, M.M., Moss, H.B., Yu, L.M., Tarter, R.E., and Deka, R. (1995). Preliminary evidence for an association of a dinucleotide repeat polymorphism at the MAOA gene with early onset alcoholism/substance abuse. Am. J. Med. Genet. *60*, 122–126.
20. Hsu, Y.-P., Loh, E., Chen, W., Chen, C.-C., Yu, J.-M., and Cheng, A.T. (1996). Association of monoamine oxidase A alleles with alcoholism among male Chinese in Taiwan. Am. J. Psychiatry *153*, 1209–1211.
21. Castagné, V., Moser, P., Roux, S., and Porsolt, R.D. (2007). Rodent models of depression: Forced swim and tail suspension behavioral despair tests in rats and mice. Current Protocols in Pharmacology (Supplement 38).
22. Renard, C.E., Dailly, E., David, D.J., Hascoet, M., and Bourin, M. (2003). Monoamine metabolism changes following the mouse forced swimming test but not the tail suspension test. Fundam. Clin. Pharmacol. *17*, 449–455.
23. Zheng, B., Larkin, D.W., Albrecht, U., Sun, Z.S., Sage, M., Eichele, G., Lee, C.C., and Bradley, A. (1999). The *mPer2* gene encodes a functional component of the mammalian circadian clock. Nature *400*, 169–173.

Supplemental Data

Animals

Wild-type and *Per2*^{Brdm1} mutant littermates [S1] were derived from heterozygous *Per2*^{Brdm1} mutant breeding pairs and housed under a 12 hr light/12 hr dark regimen (Zeitgeber time [ZT] 0 = time when lights go on). Three- to six-month-old males were used for experiments. Animal care and handling was performed according to the Canton of Fribourg's law for animal protection authorized by the Office Veterinaire Cantonal de Fribourg. The in vivo electrophysiology experiments were performed under the approval of the Animal Experiments Ethical Committee of the Leiden University Medical Center.

Luciferase Reporter Assays and Transfections

A 1.1 kb or a 0.7 kb fragment of the mouse monoamine oxidase A (Maoa) promoter region (nucleotides −974 to +144 or −607 to +144 of transcriptional start site, respectively) or a 1.2 kb fragment of mouse monoamine oxidase B (Maob) promoter region (−1230 to +35 of transcription start site) was cloned into the pGL3 basic vector (Promega, Madison, WI) containing the firefly luciferase reporter gene. Full-length mouse cDNAs encoding mBmal1 (BC_011080), mNpas2 (BC_ 109166), mClock (AF_000998), mPer2 (AF_036893), and bacterial β-galactosidase (NC_009800) were cloned into pSCT1 [S2]. For the expression of mCry1 (AF_156986), the full-length mouse cDNAs were cloned into pSTC-TK, an expression vector similar to pSCT1, which additionally contains a thymidine kinase leader sequence after the CMV promoter. Two mammalian cell lines were used for cotransfection studies: NG108-15 (Mouse neuroblastoma × Rat glioma hybrid) [S3] and COS-7 (kidney cells of the African green monkey). Cells were maintained in Dulbecco's modified Eagle medium (DMEM) supplemented with 10% fetal-calf serum and 100 U/ml of penicillin and streptomycin. Proliferating cells were transfected with same quantities of either reporter plasmid (0.5 μg of the 1.1 kb fragment of the m*Maoa* promoter, 0.48 μg of the 0.7 kb fragment of the m*Maoa* promoter, or 0.4 μg of the empty reporter plasmid) with JetPEI transfection reagent (Polyplus Transfection, Illkirch Cedex, France). As a positive control, we used 0.1 μg of the *mPer1* 7.2K promoter [S4]. Amounts of the expression plasmids added were as follows: 0.8 μg for BMAL1, NPAS2, and CLOCK, 0.1 μg for mCRY1 and β-galactosidase, and 1 μg for PER2. The total amount of expression plasmid was adjusted to 2.6 μg by an addition of the empty pSCT1 expression plasmid. Twenty-four to thirty-two hours after transfection, luciferase activity was measured according to [S5] during a 10 s interval in a MicroLumatPlus luminometer (Berthold Technologies, Bad Wildbach, Germany). We normalized luciferase activity for transfection efficiency by determining the β-galactosidase activity of the cotransfected β-galactosidase expression plasmid. β-galactosidase activity was measured with a fluorescent-substrate-based assay as described in [S6]. Fluorescence was measured at 360 nm excitation and 460 nm emission wavelength in a Lambda Fluoro 320 fluorimeter (MWG Biotech, Ebersberg, Germany). Data are plotted as luciferase activity divided by β-galactosidase activity derived from the same sample.

Real-Time Bioluminescence Monitoring

Proliferating NG108-15 or NIH 3T3 cells in 35 mm culture dishes were transfected with 1.9 μg (0.5 μg for NIH 3T3) of the luciferase reporter constructs and 0.05 μg of a control construct expressing secreted alkaline phosphatase (SEAP, Clontech, Mountain View, California) under the control of a CMV promoter with JetPEI transfection reagent (Polyplus Transfection). The luciferase construct pGL3+2,398.luc [S7] that contains oligomerized E-box motifs (n = 4) derived from intron 2 of the *mDbp* gene was used as a positive control for the experiments. Cells were synchronized 48 hr after transfection by addition of DMEM containing 100 nM dexamethasone as described previously [S8]. After 20 min, the medium was changed to phenol red-free DMEM supplemented with 0.1 mM luciferin and 10% FCS. Bioluminescence was continuously monitored (LumiCycle, Actimetrics, Wilmette, Illinois). Bioluminescence recordings were analyzed with LumiCycle analysis software (Actimetrics). We performed trend elimination by fitting a polynomial trend (order of four) to the raw data. Data were then normalized to the secreted alkaline phosphatase activity (Roche Applied Science, Rotkreuz, Switzerland) in the culture medium taken before synchronization.

Chromatin Immunoprecipitation

Individual 3-mm-wide brain sections from five mice encompassing the *substantia nigra* and ventral tegmental area regions were combined per time point, homogenized in 1% formaldehyde/1× PBS, and kept for 5 min at 25°C. Nuclei and soluble chromatin fragments were obtained by ultracentrifugation and sonification according to a published procedure for liver tissue [S9] and precipitated with an antibody raised against BMAL1 protein (gift from U. Schibler, Geneva); coimmunoprecipitated DNA was quantified with TaqMan real-time PCR and the primers described in the Table 2 (Table S2). Shown is the amount of coimmunoprecipitated DNA related to the starting material (percent of input).

In Situ Hybridization

Mice were sacrificed at Zeitgeber times 0, 6, 12, and 18. Specimen preparation, ^{35}S-UTP-labeled riboprobe synthesis, and hybridization steps were performed as described [S10].

The in situ hybridization probes were made from cDNAs corresponding to nucleotides 55–606 of *mMaoa* (NM_173740), nucleotides 895–1626 of *mMaob* (NM_172778), nucleotides 988–1812 of *mDrd1A* (NM_010076), nucleotides 579–1371 of *Drd2* (NM_010077), and nucleotides 265–878 of *mDat* (NM_010020). The oligonucleotides used for cloning these probes are shown in Table S3. We verified specificity of the probes by hybridizing sense- and antisense-labeled transcripts. Mesolimbic brain regions were defined according to [S11].

We performed quantification of the signals from the VTA, LC, and Sn regions by densitometric analysis (GS-700 or GS-800, BioRad, Hercules, California) of autoradiograph films (Amersham Hyperfilm MP, GE Healthcare, Chalfont St. Giles, United Kingdom) with "Molecular Analyst" or "Quantity One 1-D" analysis software (BioRad). From these, we subtracted the background as found in an adjacent brain area. For each time point and genotype, three animals were used and three to six sections per brain region were analyzed. We assessed the "relative mRNA abundance" values of every gene and brain region by defining the highest value of each experiment in wild-type animals as 100%.

Monoamine Oxidase Activity Measurement

mMAO activity was measured in mitochondrial protein extracts with the luminescent MAO-Glo assay kit (Promega Corp) according to the manufacturer's instructions. In brief, mouse brains were taken at four different ZTs and frozen in liquid nitrogen. Regions corresponding to *striatum* or VTA/*Sn* were dissected, and mitochondrial proteins were isolated by sequential centrifugation. Total MAO activity was assayed by incubation of 5 μg of mitochondrial protein extract (70 mM sucrose, 230 mM mannitol, 1 mM EDTA [pH 7.0], 10 mM Tris-HCl [pH 7.5], and 1× protease inhibitor cocktail [Roche Applied Science]) for 20 min at 35°C. Total MAO activity is plotted as RLU/mg protein/min.

HPLC Analysis of Brain Tissue

Frozen brains from adult animals were dissected into different brain areas on a cold plate (−15°C). Samples were weighed and stored at −80°C until homogenization. Coronal slices of striatum (CPu plus NAc) were cut from frozen mouse brains after removal of the cortical areas lateral, medial, and dorsal from forceps minor of corpus callosum as well as the areas central from the commissura anterior. For orientation, Bregma 1.54 mm −0.14 mm according to "The mouse brain in stereotaxic coordinates" [S11] were used. Samples were weighed and stored at −80°C until homogenization. Each frozen tissue sample was homogenized by ultrasonication in

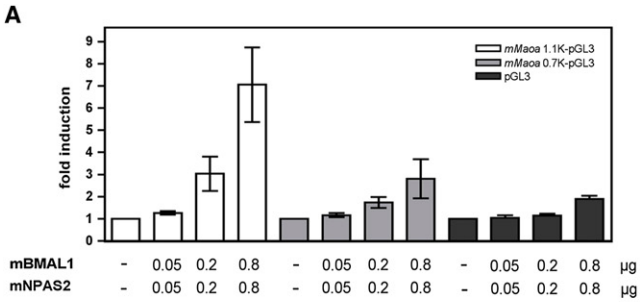

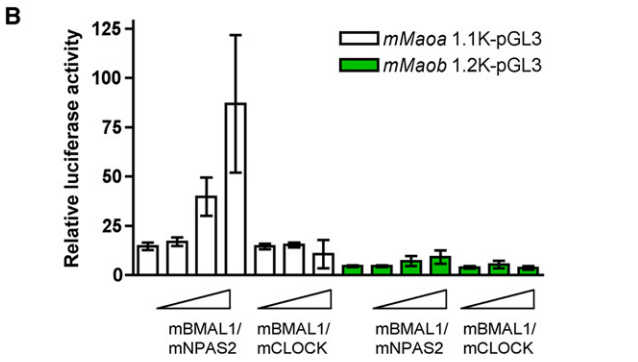

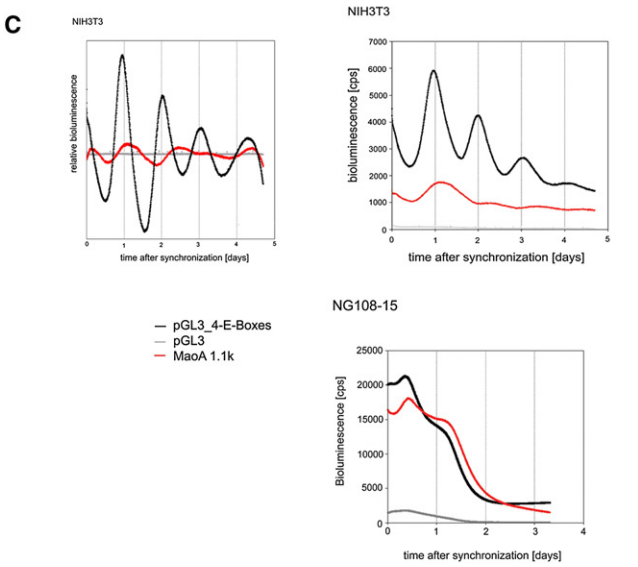

Figure S1. Activation of *mMaoa* and *mMaob* Promoters by Clock Factors in NG108-15 Neuroblastoma Cells

(A) Dose-dependent activation of transcription by mBMAL1 and mNPAS2 of the 1.1 kb *mMaoa* promoter (white bars) and the 0.7 kb *mMaoa* promoter (gray bars) with the canonical E-box deleted. Vector pGL3 control (black bars) is shown. Fold induction represents relative luciferase activity of reporter with expression plasmids (BMAL1 and NPAS2) divided by luciferase activity of reporter without expression plasmids.

(B) A total of 0.05 µg, 0.2 µg, and 0.8 µg of expression plasmids (triangle ramps) encoding for murine *Bmal1*, *Npas2*, or *Clock* were added in equal amounts to 0.5 µg of *mMaoa* (white bars) or *mMaob* (gray bars) luciferase reporter constructs containing 1.1 kb and 1.2 kb of the corresponding promoter, respectively. Two-way ANOVA with Bonferroni post test revealed significant differences for dose-dependent induction of transcription by mBMAL1/mNPAS2 for *mMaoa* ($p < 0.01$). mBMAL1/CLOCK failed to activate transcription of *mMaoa* ($p > 0.05$). No significant activation of transcription for *mMaob* neither by mBMAL1/mNPAS2 nor by mBMAL1/mCLOCK was observed ($p > 0.05$) as compared to the construct with no expression plasmids. Each value represents the mean ± SD of three independent experiments with three replicates for each experiment.

(C) Circadian oscillations of luciferase reporter activity in dexamethasone synchronized NIH 3T3 or NG108-15 cells. Shown are raw bioluminescence profiles (cps) (right panels) or detrended time series (relative bioluminescence) (left panel), each derived by averaging the normalized bioluminescence profiles of two independent cultures (representative experiment out of three independent experiments). "pGL3" represents luciferase reporter (gray, negative control), "pGL3_4-E-box" represents pGL3 reporter containing four E-boxes of the *Dbp* promoter (black, positive control), "Maoa 1.1k" represents pGL3 reporter containing a 1.1 kb promoter fragment of the mouse *Maoa* promoter (red line).

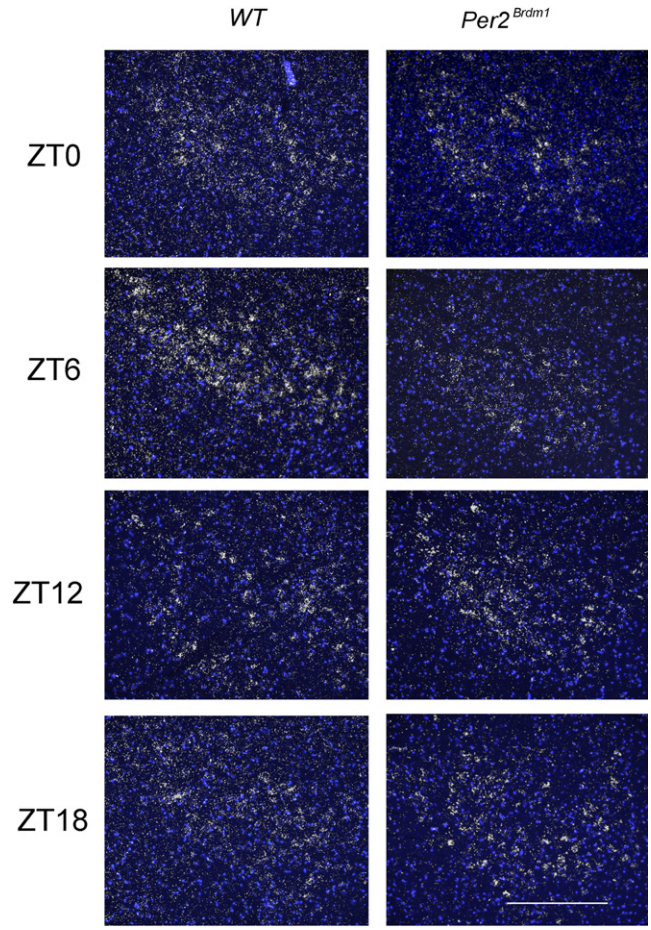

Figure S2. Representative Photomicrographs of *mMaoa* mRNA Expression in the VTA of Wild-Type and *Per2*^{Brdm1} Mutant Mice at Different Time Points

The blue color represents Hoechst stained nuclei and white represents *mMaoa* transcripts in the right hemisphere of the brain. Scale bar: 500 µm.

10–20 volume of deionized water at 4°C. Immediately after sonication, an aliquot of the homogenate (200–300 µl) was added to an equal volume of 0.2 N perchloric acid and centrifuged at 25,000 × g for 10 min at 4°C. The supernatant was used for the measurements of dopamine, DOPAC, and serotonin.

Microdialysis

Five- to six-month-old male *Per2*^{Brdm1} mutant mice (n = 8) and their respective littermates (n = 8) were single housed with food and water ad libitum and maintained in a 12 hr/12 hr light-dark cycle (lights on from 7–19 hr). Surgeries were performed under gas anesthesia, with 4% isoflurane inhalation with oxygen as the carrier gaz. Mice were mounted in a Cunningham stereotaxic

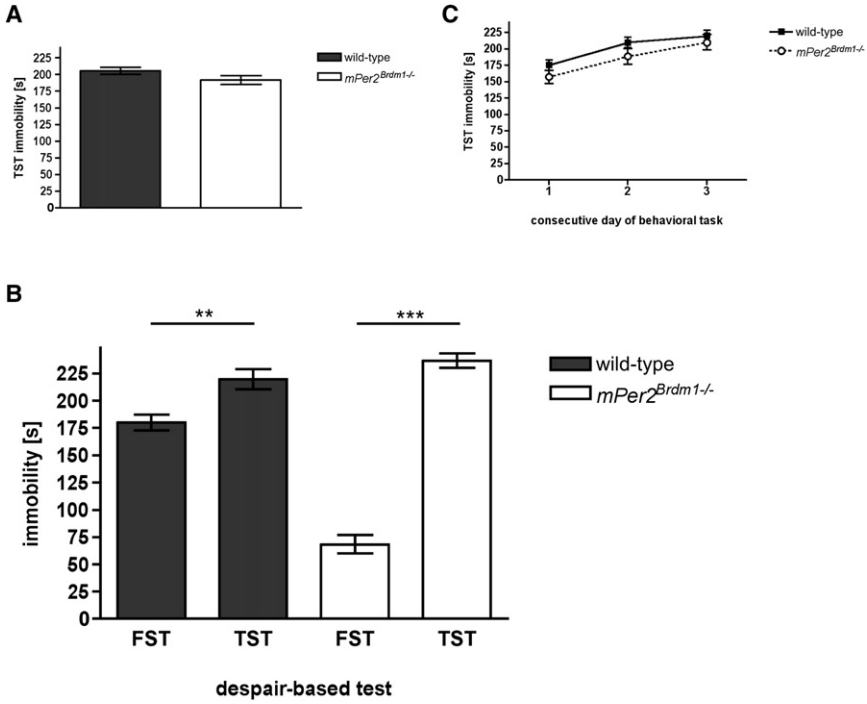

Figure S3. Immobility Times in the Tail Suspension Test and the Forced Swim Test

(A) Mean ± SEM of 36 animals tested on 3 consecutive days. No significant differences between the genotypes were observed by one-tailed unpaired t test ($p > 0.05$). Data for wild-type (black) and *Per2*^{Brdm1} mutant mice (white) at ZT 6 are shown.

(B) TST immobility plotted by day. Two-way ANOVA with Bonferroni post test revealed no difference between genotypes for each day ($p > 0.05$). Variation between days was significantly different ($p < 0.0001$).

(C) Comparison of the two genotypes in the FST and TST. Data are plotted as mean ± SEM of six animals per genotype with three test sessions on consecutive days per behavioral test. Two-way ANOVA with Bonferroni post test revealed higher immobility times for TST in both genotypes (**$p < 0.01$ for wild-type and ***$p < 0.001$ for *Per2*^{Brdm1} mutant mice). Only FST immobility times differ between genotypes ($p < 0.001$). The source of variation was significantly different for genotype, despair-based test, and interaction between the two parameters (all $p < 0.0001$).

mice adaptor device (Stoelting, Wood Dale, Illinois). Mice were implanted unilaterally with a CMA7 guide cannula (CMA Microdialysis, Stockolm, Sweden) aiming at the ventral striatum with the following coordinates: +1.2 mm posterior, +1.3 mm lateral, and −3.0 mm ventral from bregma. Guide cannulas were fixed to the brain with two anchor screws and dental cement. After surgery, mice were placed back in their home cage, but the grid cover was replaced by a Plexiglas cage-extension (height: 20 cm). Seven days after surgeries, CMA7/1 microdialysis probes of 1 mm membrane length (CMA Microdialysis AB, Stockolm, Sweden) were slowly inserted in the ventral striatum through the guide cannulas, and mice were connected to a single-channel liquid swivel and a counterbalancing system (Instech Laboratories, Plymouth Meeting, Pennsylvania). Microdialysis probes were perfused with sterile artifical cerebro-spinal fluid (CMA Microdialysis AB) at a flow rate of 1 μl/min with a PHD2000 microinfusion pump (Harvard Apparatus, Holliston, Massachusetts). After overnight stabilization, the sampling period started at 9 a.m. and stopped 24 hr later. Microdialysis samples were collected every 30 min in 300 μl plastic tubes containing 6 μl of 100 mM $HClO_4$ for stabilization and stored in – 80°C until HPLC analysis. Mouse brains were frozen in an isopentane solution, and probe placements were verified histologically on microsections of 50 μm. HPLC analysis was performed as follows: DA content in the dialysate samples was determined by high-pressure liquid chromatography. Electrochemical detection was acquired with the ALEXIS 100 cooled-micro LC-EC system (Antec Leyden bv, Zoeterwoude, The Netherlands) equipped with a microbore VT-03 flow cell. The working potential of the cell was set at 400mV, and the oven temperature of the DECADE II was set at 35°C. The mobile phase of pH 6 contained 50 mM phosphoric acid, 400 mg/l OSA, 0.1 mM EDTA, 8 mM KCl, and 15% methanol and was perfused with a flow rate of 200 μl/min. Duplicates of 4 μl aliquots of each sample were injected onto a reversed phase column (C18, ALF-205 column, 50× 2.1mm ID, 3 μm; Axel Semrau GmbH & Co. KG, Sprockhövel, Germany), and the DA content was determined with the area under the peak and an external standard curve as a reference. Detection limits for DA was 250 pM with a signal-to-noise ratio of 2. All data were analyzed with a one- or two-way ANOVA for repeated measures. Data presented are mean ± SEM.

Porsolt Forced-Swim Test

Animals were placed in a cylindrical tank (35 cm high, 25 cm in diameter) filled with water of 25°C–30°C up to a height of 20 cm. After a habituation period of 2 min, immobility behavior was assessed during a period of 4 min. Total time spent floating in an immobile position (no visible body or limb movements [S12]) was measured with a stopwatch. Values are plotted as cumulative immobility times in seconds.

Tail-Suspension Test

The tail-suspension test was conducted according to the EMPRESS standard operating procedure (http://empress.har.mrc.ac.uk).

In brief, mice were suspended individually at the tail with a cord in a white box (36.5 cm high, 30.5 × 30.5 cm^2). Animals were judged to be in an immobile posture when they stopped agitation or stopped to attempt to escape. Immobility was recorded for six minutes with a stopwatch. All values are plotted as cumulative immobility times in seconds [S13, S14].

Drug Treatments

Animals were habituated three to four times to the behavioral task before drug injection. DL-alpha-methyl-p-tyrosine (AMPT) was purchased from ACROS ORGANICS (Geel, Belgium). Amitryptiline hydrochloride (AMI) and trans-2-Phenylcyclopropyl-amine hydrochloride (TCP) were purchased from Sigma (Buchs, Switzerland). All drugs tested were dissolved in sterile saline. For the AMPT injections, the mice received i.p. a dose of 200 mg/kg at ZT 6, 1 hr before the performance of the FST. For the antidepressant treatment, we administered the drug 30 min before the behavioral task in groups of six animals per genotype around ZT 6 [S15]. We injected doses of 3 mg/kg, 6 mg/kg, and 9 mg/kg AMI and 6 mg/kg, 9 mg/kg, and 12 mg of TCP to see whether the anti-immobility effect of the injected antidepressants shows a dose dependence [S16]. All values are plotted as the cumulative immobility times in seconds. For the delta TST immobility, we subtracted the value of the pharmacological treatment from the corresponding value of the saline injection of the day before the pharmacological treatment. We performed statistical analysis of the data by comparison of the medians of wild-type and *Per2*^{Brdm1} mutant animals by using the Mann-Whitney test.

In Vivo Multiunit Recording

Wild-type C57Bl/6 (Harlan, The Netherlands), homozygous *Per2*^{Brdm1} mutant mice and wild-type littermate animals were brought under Midazolam/Fentanyl/Fluanisone anesthesia and stereotactically implanted with a tripolar stainless-steel electrode (125, Plastics One, Roanoke, Virginia), which was fixed to the skull. Two electrodes were insulated and twisted together with only the tips exposed and aimed at the left ACb. Under a 5° angle in the coronal plane, the electrodes were placed 1.34 mm anterior to bregma, 1.1 mm lateral to the midline, and 3.9 mm ventral to the surface of the cortex. The third, uninsulated electrode was placed in the cortex for reference. After the implantation, the animals were housed individually. After a recovery period of at least 7 days, the animals were transferred to the recording setup and the electrode was connected to the recording hardware via a counterbalanced swivel system. The animals could move freely through their cage throughout the recording. Behavioral activity was monitored by means of a passive infrared movement detector. The signal from

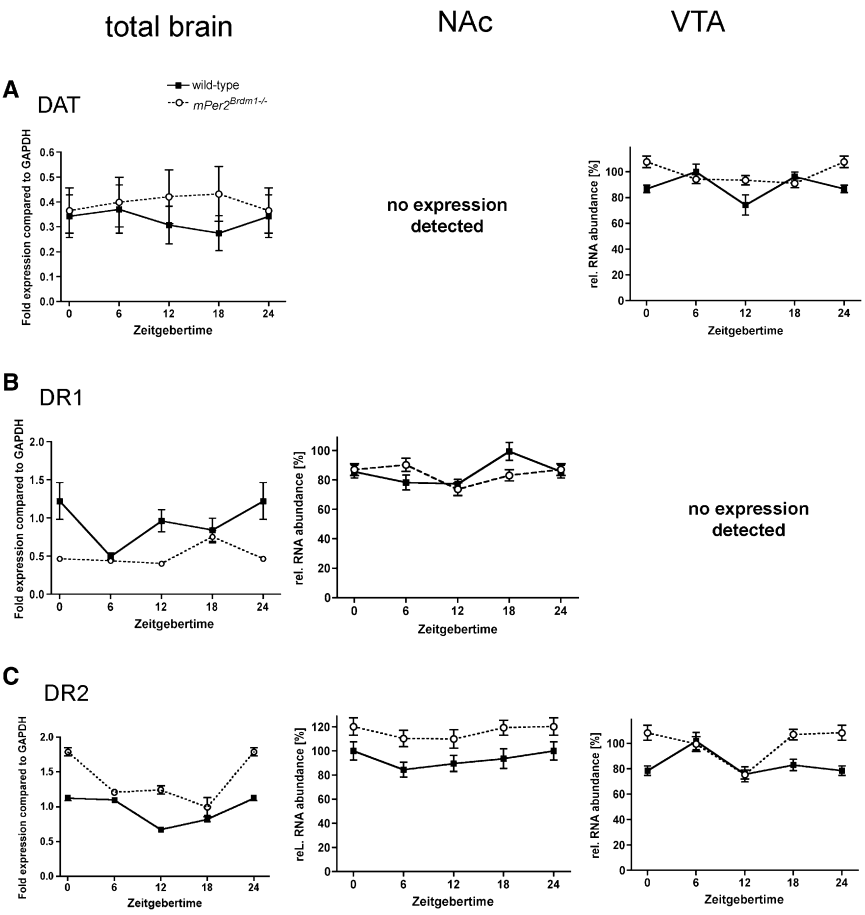

Figure S4. Expression of Dopamine Transporter, Dopamine Receptor 1, and Dopamine Receptor 2

Expression analysis in total brain was performed with quantitative PCR. Expression in the NAc and VTA was determined by in situ hybridization. The following abbreviations are used: DAT, Dopamine Transporter; DR1, Dopamine Receptor 1; and DR2, Dopamine Receptor 2.

(A) DAT expression. For total brain, two-way ANOVA revealed no effect on genotype ($p > 0.05$) and time ($p > 0.05$) and no interaction between the two ($p > 0.05$). In the NAc, no expression was detected. In the VTA, two-way ANOVA revealed an effect on genotype ($p < 0.001$) and time ($p < 0.01$) and interaction between the two ($p < 0.01$). Bonferroni post test indicates significant differences between the genotypes at ZT 0/24 and ZT 12.

(B) Expression of DR1. For total brain, two-way ANOVA revealed an effect on gentoype ($p < 0.001$) and time ($p < 0.05$) and interaction between the two ($p < 0.01$). Bonferroni post test revealed significant differences at ZT 0/24 and ZT 12. In the NAc, two-way ANOVA revealed no effect on genotype ($p > 0.05$) but an effect on time ($p < 0.05$) and interaction between the two ($p < 0.05$). Bonferroni post test revealed no significant differences. In the VTA, no expression was detected.

(C) Expression of DR2. For total brain, two-way ANOVA revealed an effect on genotype ($p < 0.001$) and time ($p < 0.001$) and interaction between the two ($p < 0.001$). Bonferroni post test revealed significant differences at ZT 0/24 and ZT 12. In the NAc, two-way ANOVA revealed an effect on genotype ($p < 0.0001$) but not on time ($p > 0.05$) and no interaction between the two ($p > 0.05$). Bonferroni post test reveals no significant differences. In the VTA, two-way ANOVA revealed an effect on genotype ($p < 0.0001$) and time ($p < 0.0001$) and interaction between the two ($p < 0.001$). Bonferroni post test reveals significant differences at ZT 0/24 and ZT 18. ZT 0 and 24 are identical and are double plotted in all experiments.

Table S1. Maoa-Reporter Activation in Neuroblastoma and COS-7 Cells

		Relative Luciferase Activity[a] (mean ± SEM)		Fold Induction[b] (mean ± SEM)	
		Cotransfected Clock Genes in Expression Plasmid			
Cell Line	Reporter Plasmid	+0.8 μg mBMAL1/ mNPAS2	+0.8 μg mBMAL1/ mCLOCK	+0.8 μg mBMAL1/ mNPAS2	+0.8 μg mBMAL1/ mCLOCK
NG108-15					
	mMaoa −1.1K-pGL3	211.8 ± 10.56	25.32 ± 1.166	3.726 ± 0.2682	0.8627 ± 0.1058
	pGL3[c]	7.773 ± 0.7192	3.557 ± 0.2679	1	1
	mPer1 −7.2K-pGL3	3014 ± 289.6	749.4 ± 94.51	5.176 ± 0.3968	2.987 ± 0.4456
	pGL3[d]	8.689 ± 1.240	3.285 ± 0.5019	1	1
COS-7					
	mMaoa −1.1K-pGL3	62.76 ± 14.20	9.448 ± 2.098	2.602 ± 0.1476	2.012 ± 0.1588
	pGL3[3]	4.012 ± 1.204	0.7384 ± 0.2644	1	1
	mPer1 −7.2K-pGL3	605.9 ± 49.20	242.3 ± 16.13	8.357 ± 0.7428	19.60 ± 2.406
	pGL3[d]	7.067 ± 1.202	1.448 ± 0.3314	1	1

[a] Relative luciferase activity refers to luciferase activity of reporter plasmid divided by β-galactosidase activity (of cotransfected lacZ expression plasmid).
[b] Fold induction: To obtain these values, we calculated first the values named "(normalized to the emtpy reporter)." Therefore, we divided the values of the relative luciferase activity of the promoter-pGL3 construct by the corresponding relative luciferase activity of the empty reporter plasmid (pGL3 basic vector) cotransfected either with the same clock-gene expression plasmids as the promoter-pGL3 construct or without any clock-gene expression plasmids. The values of the relative luciferase activity of the promoter-pGL3 constructs and of the empty reporter plasmid respectively cotransfected without any clock-gene expression plasmids are not listed the table above. Subsequently, we divided these "(normalized to the empty reporter)" values of the promoter-pGL3 construct cotransfected with clock-gene expression plasmids by the "(normalized to the empty reporter)" values of the promoter-pGL3 construct without any cotransfected clock genes in expression plasmids.
[c] Transfected in parallel in the same experiments as with *mMaoa* promoter −1.1K-pGL3 construct and cotransfected with the same clock-gene expression plasmids as the promoter construct pGL3.
[d] Transfected in parallel in the same experiments as with *mPer1* promoter −7.2K-pGL3 construct and cotransfected with the same clock-gene expression plasmids as the promoter construct pGL3.

Table S2. Primers and Probes for Real-Time PCR

Primer Name	Sequence
RevErbα_FW	5′-TCA TGC CCT CTT TCA GGA TT-3′
RevErbα_RV	5′-TTA CCC GGC TAT GGT TTC AC-3′
RevErbα_TM	5′-FAM-TAA CCC ATC CTC CAA CCC AGC C-BHQ1-3′
Maoa_FW	5′-GTA GCT CTG CCA GCT CGT TC-3′
Maoa_RV	5′-CCT GAA TGG ATT CGT TCG TC-3′
Maoa_TM	5′-FAM-CGG ACC GTC TCC CAA CCC CT-BHQ1-3′
Bmal1_FW	5′-CAG CGA GCC ACG GTG A-3′
Bmal1_RV	5′-CCC GAG ACG GCT GCT-3′
Bmal1_TM	5′-FAM-CCG CAG CCA TGC CGA CAC-BHQ1-3′

FAM, 6-flourescine; BHQ1, black hole quencher 1.

the electrodes was differentially amplified and filtered before being fed into window discriminators. The window discriminators convert action potentials with an amplitude that falls between an upper and a lower voltage threshold into pulses. The pulses were counted in 10 s bins and stored on a computer for offline analysis. The first day after the start of the recording the animals received a saline (control) injection at ZT 6. The next day at ZT 6, they received an AMI injection at a dose of 9 mg/kg body weight. A day later, they were disconnected from the setup and transferred to their home cage. After at least 14 days, the animals were reconnected to the recording system and received an injection of TCP at ZT 6 (6 mg/kg body weight).

Analysis

As visible in Figures 4A–4D, the electrical activity we measured from the NAc displayed a baseline firing rate, interspersed by bouts of higher electrical activity that correlated with locomotor activity as measured by passive-infrared movement detectors (data not shown). Because the animals became relatively inactive after AMI and TCP injections, we compared the MUA during the maximal response with baseline MUA that was recorded when animals were inactive. We quantified the response by taking the mean MUA over 5 min intervals for the last three hours prior to the time of injection, and compared stable mean values to the averages from a 5 min epoch of MUA taken during the maximum of the response. When no clear response was visible, we measured the mean MUA over 5 min intervals for the first three hours after the time of injection. We calculated the magnitude of the response by normalizing the baseline and response values to the baseline value and calculating the difference.

Supplemental References

S1. Zheng, B., Larkin, D.W., Albrecht, U., Sun, Z.S., Sage, M., Eichele, G., Lee, C.C., and Bradley, A. (1999). The *mPer2* gene encodes a functional component of the mammalian circadian clock. Nature *400*, 169–173.

S2. Wieland, S., Dobbeling, U., and Rusconi, S. (1991). Interference and synergism of glucocorticoid receptor and octamer factors. EMBO J. *10*, 2513–2521.

S3. Yujnovsky, I., Hirayama, J., Doi, M., Borrelli, E., and Sassone-Corsi, P. (2006). Signaling mediated by the dopamine D2 receptor potentiates circadian regulation by CLOCK:BMAL1. Proc. Natl. Acad. Sci. USA *103*, 6386–6391.

S4. Yamaguchi, S., Mitsui, S., Miyake, S., Yan, L., Onishi, H., Yagita, K., Suzuki, M., Shibata, S., Kobayashi, M., and Okamura, H. (2000). The 5′ upstream region of mPer1 gene contains two promoters and is responsible for circadian oscillation. Curr. Biol. *10*, 873–876.

S5. Miranda, M., Majumder, S., Wiekowski, M., and DePamphilis, M. (1993). Application of firefly luciferase to preimplantation development. Methods Enzymol. *255*, 412–433.

S6. Jain, V.K., and Magrath, I.V. (1991). A chemiluminescent assay for quantitation of beta-galactosidase in the femtogram range: Application to quantitation of beta-galactosidase in lacZ-transfected cells. Anal. Biochem. *199*, 119–124.

S7. Ripperger, J.A., Shearman, L.P., Reppert, S.M., and Schibler, U. (2000). CLOCK, an essential pacemaker component, controls expression of the circadian transcription factor DBP. Genes Dev. *14*, 679–689.

S8. Balsalobre, A., Brown, S.A., Marcacci, L., Tronche, F., Kellendonk, C., Reichardt, H.M., Schutz, G., and Schibler, U. (2000). Resetting of circadian time in peripheral tissues by glucocorticoid signaling. Science *289*, 2344–2347.

S9. Ripperger, J.A., and Schibler, U. (2006). Rhythmic CLOCK-BMAL1 binding to multiple E-box motifs drives circadian Dbp transcription and chromatin transitions. Nat. Genet. *38*, 369–374.

S10. Albrecht, U., Lu, H.-C., Revelli, J.-P., Xu, X.-C., Lotan, R., and Eichele, G. (1998). Studying gene expression on tissue sections using *in situ*, hybridization. In Human Genome Methods, K.W. Adolph, ed. (Boca Raton: CRC Press), pp. 93–120.

S11. Paxinos, G., and Franklin, K. (2001). The Mouse Brain in Stereotaxic Coordinates, Second Edition (San Diego: Academic Press).

S12. Porsolt, R.D., Le Pichon, M., and Jalfre, M. (1977). Depression a new animal model sensitive to antidepressant treatments. Nature *266*, 730–732.

S13. Dalvi, A., and Lucki, I. (1999). Murine models of depression. Psychopharmacology (Berl.) *147*, 14–16.

S14. Liu, X., and Gershenfeld, H.K. (2001). Genetic differences in the tail-suspension test and its relationship to imipramine response among 11 inbred strains of mice. Biol. Psychiatry *49*, 575–581.

S15. Heurteaux, C., Lucas, G., Guy, N., El Yacoubi, M., Thummler, S., Peng, X.D., Noble, F., Blondeau, N., Widmann, C., Borsotto, M., et al. (2006). Deletion of the background potassium channel TREK-1 results in a depression-resistant phenotype. Nat. Neurosci. *9*, 1134–1141.

S16. Ushijima, K., Sakaguchi, H., Sato, Y., To, H., Koyanagi, S., Higuchi, S., and Ohdo, S. (2005). Chronopharmacological study of antidepressants in forced swimming test of mice. J. Pharmacol. Exp. Ther. *315*, 764–770.

Table S3. Oligonucleotides for ISH Probes

Primer Name	Sequence
mMaoa Sense	5′-GAC TTC AGT CAA GGG GCG GTA C-3′
mMaoa Antisense	5′-CTT GTC CCA TTC CTC AGA TGT CTT G-3′
mMaob Sense	5′-GGC ATG AAG ATT CAC TAT AGT CCT CC-3′
mMaob Antisense	5′-GTG GGC CAG GAA ACC AAG AGC-3′
mDrd1A Sense	5′-CAG TGC AGC TAA GCT GGC ACA AG-3′
mDrd1A Antisense	5′-GAG AGA CAT CGG TGT CAT AGT CC-3′
mDrd2 Sense	5′-CCG AGT TAC TGT CAT GAT CGC C-3′
mDrd2 Antisense	5′-CCA TGT GAA GGC GCT GTA GAG G-3′
mDat Sense	5′-GCA GAA TGG AGT GCA GCT GAC C-3′
mDat Antisense	5′-CTG TGA GCT GCC ACC GTG GAG-3′